J. Micromech. Microeng. **23** (2013) 035006 (7pp) doi:10.1088/0960-1317/23/3/035006

Microfabrication of air core power inductors with metal-encapsulated polymer vias

Jungkwun Kim, Florian Herrault, Xuehong Yu, Minsoo Kim, Richard H Shafer and Mark G Allen

School of Electrical and Computer Engineering, Georgia Institute of Technology, Atlanta, GA 30332, USA

E-mail: jkim831@gatech.edu

Received 29 August 2012, in final form 12 December 2012
Published 25 January 2013
Online at stacks.iop.org/JMM/23/035006

Abstract

This paper reports three-dimensional (3-D) microfabricated toroidal inductors intended for power electronics applications. A key fabrication advance is the exploitation of thick metal encapsulation of polymer pillars to form a vertical via interconnections. The radial conductors of the toroidal inductor are formed by conventional plating-through-mold techniques, while the vertical windings (up to 650 μm in height) are formed by polymer cores with metal plated on their external surfaces. This encapsulated polymer approach not only significantly reduces the required plating time but also exploits the relative ease of fabricating high-aspect-ratio SU-8 pillars. To form the top radial conductors, non-photopatternable SU-8 is introduced as a thick sacrificial layer. Two toroidal inductor geometries were fabricated and tested. The first inductor had an inner diameter of 2 mm, an outer diameter of 6 mm, 25 turns and a vertical via height of 650 μm. The second inductor had an inner diameter of 4 mm, an outer diameter of 8 mm, 50 turns and a vertical via height of 650 μm. Both inductor geometries were successfully fabricated and characterized in the frequency range of 0.1−100 MHz. Characterization results of the 25- and 50-turn inductors showed an average inductance of 76 and 200 nH, a low frequency (0.1 MHz) resistance of 0.2 and 1 Ω and a quality factor of 35 and 24 at 100 MHz, respectively. Finite-element simulations of the inductors were performed and agreed with the measured results to within 8%. The turn-to-turn breakdown voltage was measured to be in excess of 800 V and currents as high as 0.5 A could be successfully carried by the inductor windings.

(Some figures may appear in colour only in the online journal)

1. Introduction

Incorporation of miniaturized integrated power conversion subsystems, such as switching converters, into electronic systems has the potential to impact overall system size, improve energy utilization and increase system functionality, especially in systems requiring multiple levels of voltage or current for operation. However, many of these power converter subsystems resist miniaturization, as the power inductor is often the largest single component within the subsystem. Although increases in switching converter operating frequency can reduce the required value of subsystem inductance (and consequently the inductor size), increases in converter losses often preclude high frequency operation. As a result, most commercial switching frequencies are in the range of 0.5−10 MHz with research being conducted to push these frequencies up to 100 MHz and beyond. In the nearer term, miniaturized inductors with sufficient inductance and power handling capability in the range of 0.5−10 MHz are of great interest [1–4]. However, the challenge is to achieve higher degrees of miniaturization in this frequency range without sacrificing inductor performance.

Microfabrication of inductors offers the potential for continued decrease in inductor size. Microfabrication

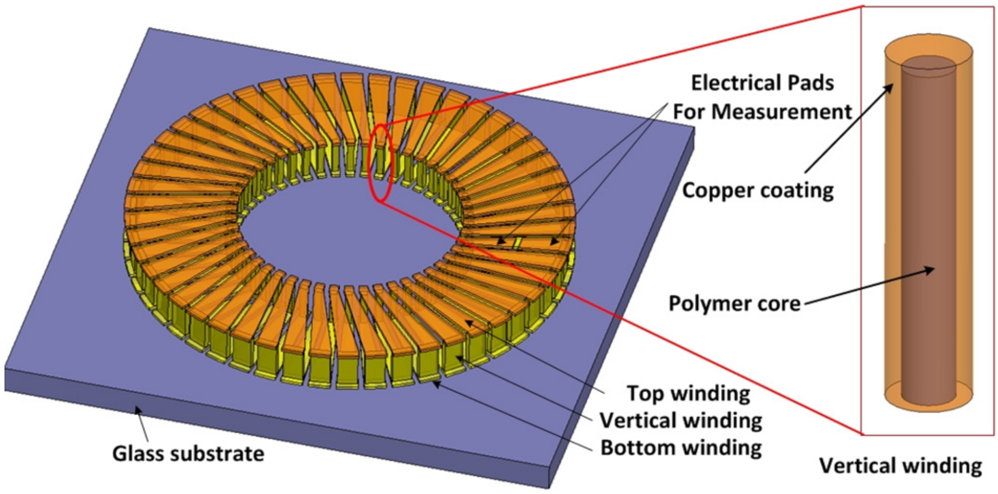

Figure 1. Schematic diagram of a 50-turn toroidal inductor and metalized polymer via as a vertical winding.

benefits include decreasing the physical size of windings, incorporating core materials with small-scale features such as sputtered nanomagnetic materials or materials with laminations and improving opportunity for co-integration with other microfabricated devices on a chip or package. Microfabrication-based compact inductors and transformers for switching converters are therefore being increasingly studied. Typical inductor geometries include racetrack [4, 5] and circular/rectangular spiral types [6–10]. Many reported microfabricated inductors possess planar geometries so as to exploit the use of well-developed planar microfabrication processes. One disadvantage of planar geometries is that relatively large external magnetic fields may be generated, especially at high power levels and for air-core devices [11–13]. These fields may cause electromagnetic interference (EMI) with other system elements and/or may induce eddy currents in nearby conductors or semiconductors.

Toroidal inductor geometries, in which the generated magnetic flux is confined within the windings, offer the potential for reduced EMI and lower loss due to stray fields. A challenge of this geometry for power applications is that the flux cross-sectional area and therefore the thickness of these inductors should be substantial. Previous miniaturized toroidal air-core inductors, including copper-winding toroids fabricated using printed circuit boards (PCB), silicon and Pyrex substrates have been demonstrated [14–18]. Often, however, these geometries possess fabrication or resolution limitations on the ultimate size and value of achievable inductance. For example, inductors fabricated using the through-mold-electroplating method [16, 19] require an extremely long electroplating time to achieve large magnetic cross-sectional areas. PCB-based toroidal inductors are limited in minimum feature size [15]. Inductors using thick resists as a winding support layer between top and bottom windings typically require long processing times; further, such resists can be challenging to remove if desired after they have been crosslinked.

In this paper, we propose a fabrication method for micromachined 3-D toroidal inductors, in which metal-encapsulated polymer vias are utilized as the vertical windings. This approach, building on previous work for RF inductors [20] but now extended to power inductors, results in greatly reduced fabrication time. By combining an SU-8 dry film process to create high aspect ratio solid polymer vias with metallization of the external surfaces of these polymer vias to create an interlayer conducting path (figure 1), both the long resist processing time and the long electroplating time for thick toroidal structures can be avoided. This method also exploits the use of non-solvent-containing, reflowed SU-8 as a fabrication material and sacrificial layer to quickly enable the formation of top radial windings. This approach also results in greatly reduced process time since the reflowed, noncrosslinked SU-8 does not require the solvent evaporation time of conventional photoresist (softbaking) and is easily removable.

2. Fabrication of 3-D toroidal inductors

A typical micromachined 3-D toroidal/solenoid inductor is composed of bottom, vertical and top windings [15–20]. The proposed design utilizes solid metal bottom and top windings, and metal-encapsulated polymer vertical windings for ease of fabrication and reduction in processing time. To illustrate the process, 25- and 50-turn toroidal inductor designs with vertical winding height of 650 μm are introduced in table 1. The 25-turn inductor has a 6 mm outer diameter and a 2 mm inner diameter; this inner diameter was chosen such that it is feasible to resolve the inner winding geometries using proximity lithography. The 50-turn inductor has an 8 mm outer diameter and a 4 mm inner diameter. A 100 μm gap between windings for both inductors has been chosen due to the constraints of proximity lithography on highly nonplanar surfaces. Winding thicknesses for bottom and top windings are chosen to be 30 μm.

The fabrication sequence for the toroidal inductors comprises three major steps and is described in figure 2. The first step is the fabrication of an SU-8 pillar array for supporting the vertical windings. A polar array of holes is patterned on chromium (Cr)-coated glass to form patterns for inner and outer winding pillars. Since additional area is available for

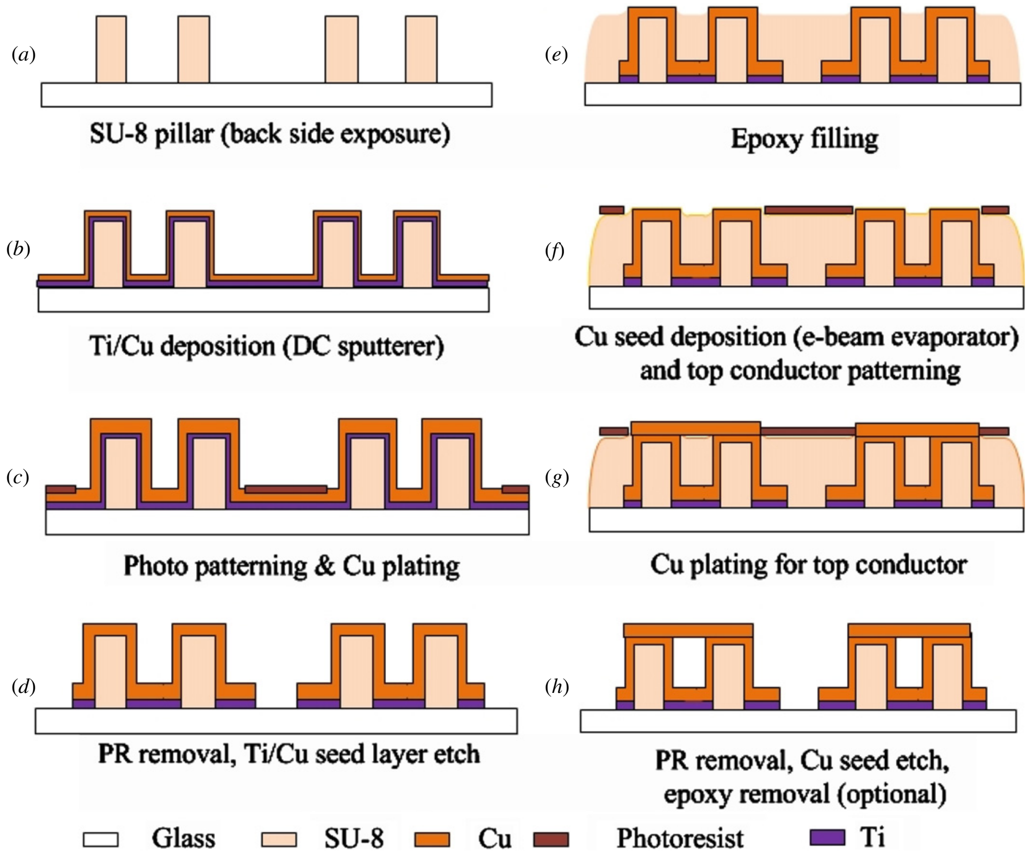

Figure 2. Fabrication process for a 3-D toroidal air core inductor.

Table 1. Specifications of 25- and 50-turn inductor models.

Number of turns	50 turns, 25 turns
Top winding	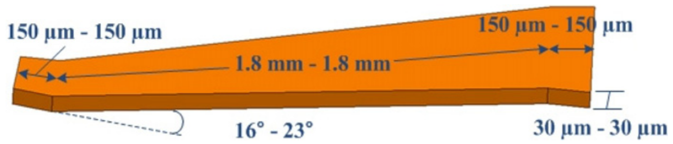
Vertical winding	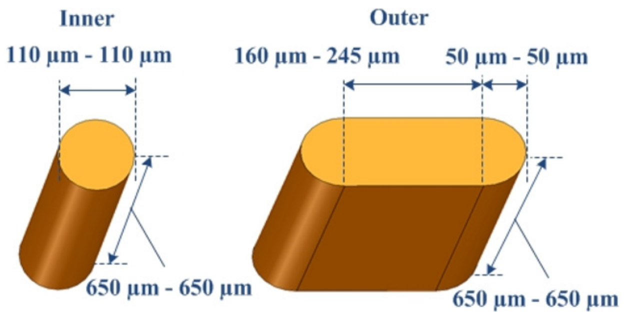
Bottom winding	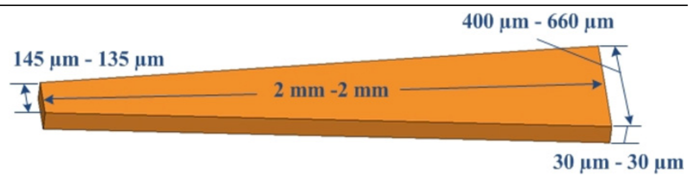
Inner diameter of the inductor	4 mm, 2 mm
Outer diameter of the inductor	8 mm, 6 mm
Winding gap	100 μm, 100 μm
Height	650 μm, 650 μm

the outer vertical windings compared to the inner vertical windings, larger ellipsoidal pillars are utilized for the outer vertical windings to minimize overall resistance. SU-8 resist must then be applied in order to form the vertical winding pillar arrays. Because substantial thicknesses of resist are required, as well as the requirement that the pillar arrays be very uniform in height, a dry film SU-8 process is employed. An SU-8 dry film (SUEX 650, DJ DevCorp.), 650 μm in thickness, is placed on the patterned Cr-coated glass and bonded for 3 min at 60 °C on a hotplate [21]. The film is exposed through the glass and patterned chromium layer using a backside exposure scheme (near UV without UV filter) with a UV light intensity of 10 mW cm^{-2} and exposure dose of 18 J (30 min exposure time) [22]. Exposure is followed by a post-exposure bake. The temperature is ramped at a rate of 6.7 °C min^{-1} to the bake temperature of 95 °C, held for 1 h and ramped down at the same rate. After baking, the sample is developed using PGMEA (propylene glycol methyl ether acetate) for 40 min and the Cr layer is removed by immersing the sample in Cr etchant (CR-7S, CYANTECK, Co.) for 1 min. After rinsing with deionized (DI) water, the SU-8 vertical winding pillar arrays are obtained (figure 2(*a*)). Fabricated SU-8 pillars comprising inner and outer vertical windings show an average positive inclined angle of 89.1° relative to the substrate, resulting in a pillar diameter difference between the base and the top of approximately 9%.

The second step is the fabrication of bottom and vertical metal windings. A seed layer of 30 nm thick titanium (Ti) and 600 nm thick copper (Cu) is deposited by dc sputtering (figure 2(*b*)). The metalized structure is spray-coated using negative photoresist NR9-1500PY (Futurrex, Inc.) to a thickness of approximately 20 μm and baked at 115 °C for 3 min. The photoresist-coated structure is patterned using proximity UV lithography (700 μm gap between mask and substrate and minimum pattern size as 100 μm) to form a mold for the bottom windings and also to expose the vertical windings (figure 2(*c*)). The photoresist is exposed with UV at an intensity of 10 mW cm^{-2} for 30 s, followed by a post-exposure bake at 95 °C for 3 min. The sample is developed (RD-6 developer, Futurrex, Inc.) for 90 s and rinsed with DI water. After an oxygen plasma descum, a Cu electrodeposition of approximately 30 μm is performed using a commercially available electrolyte (Copper Mirror Plating Solution, Shor International, Co.) with a current density of 20 mA cm^{-2} to form the bottom and vertical inductor windings simultaneously (figure 2(*d*)). The photoresist mold layers are removed by acetone and the underlying seed Ti and Cu layers are etched using a 1:10 solution of hydrofluoric (HF) acid in DI water and a 1:5 solution of hydrochloric (HCl) solution in DI water, respectively, completing the bottom and vertical windings.

The third step is the patterning of the top conductor. Non-photopatternable EPON SU-8 epoxy pellets (Miller-Stephenson, Inc.) in a quantity sufficient to form a wafer-scale film of thickness equal to the height of the electroplated vertical conductors are placed on the wafer and melted at 130 °C on a hotplate (figure 2(*e*)). Although uncrosslinked conventional SU-8 has been investigated previously as a sacrificial material [23], the use of EPON SU-8 as a sacrificial layer is attractive since not only can it be planarized at relatively low temperature, but also the lack of solvent precludes the need for extensive baking times. Further, the lack of crosslinking enables easy removal if desired. The interior volumes of the inductors as well as the field areas between inductors are thereby filled to form an almost planar surface. A Cu seed layer of 350 nm thickness is deposited using an e-beam evaporator and is coated with positive photoresist (SC1805, Shipley Company, LLC.) to a thickness of 15 μm by spray coating. An electroplating mold for the top winding pattern is formed using UV exposure (30 s, 0.9 J) and development (MF-319 developer, Shipley Company, LLC.) (figure 2(*f*)) and Cu is electrodeposited through this photoresist mold to a thickness of 30 μm (i.e. slightly overplated; figure 2(*g*)). The photoresist mold and the Cu seed layer are removed, followed by optional removal of the non-photopatternable SU-8 epoxy using acetone (figure 2(*h*)), completing the fabrication of the toroidal inductor.

Photomicrographs of the fabricated inductor at key steps during the process are shown in figure 3. A high-aspect-ratio SU-8 array of micropillars for vertical windings is shown in figure 3(*a*) and an image of inner vertical windings with a view of Cu-encapsulated SU-8 vertical windings (with some Cu removed) is shown in figure 3(*b*). Figure 3(*c*) shows an image of completed fabrication of bottom, vertical and top windings (several top windings as well as the SU-8 sacrificial material have been intentionally removed to reveal the bottom windings).

3. Results

Photomicrographs of fabricated 25 and 50 turn inductors are shown in figure 4. Figure 4(*a*) shows an overview of the 50 turn inductor and figure 4(*b*) shows an overview of the 25 turn inductor. Figure 4(*c*) shows multiple inductors fabricated on a single substrate, illustrating the batch nature of the fabrication process.

The fabricated inductors have been electrically characterized in terms of inductance, resistance and quality factor as a function of frequency as shown in figure 5 using an impedance analyzer (HP4194). Inductances of approximately 200 nH for 50-turn inductors and 76 nH for 25-turn inductors were measured over the frequency range 0.1–100 MHz (figure 5(*a*)). The ac resistance and quality factor over the same frequency range are also shown (figures 5(*b*), (*c*)). The 25-turn inductor shows an ac resistance of approximately 0.2 Ω at 0.1 MHz and a quality factor of 35 at 100 MHz. The removal of the non-photopatternable SU-8 material from the toroidal core had no significant effect on the inductor performance.

To validate the electrical characteristics of the toroidal inductor, the 3-D geometries of 25- and 50-turn inductors have been simulated using the Ansoft finite element HFSS tool. The simulated and measured inductances agree within 8% below 100 MHz. Simulation predicts a self-resonant frequency of 1300 and 860 MHz for the 25- and 50-turn inductor, respectively.

Since the fabricated inductors have been proposed for power applications, both maximum voltage and maximum current characteristics were investigated. Winding-to-winding

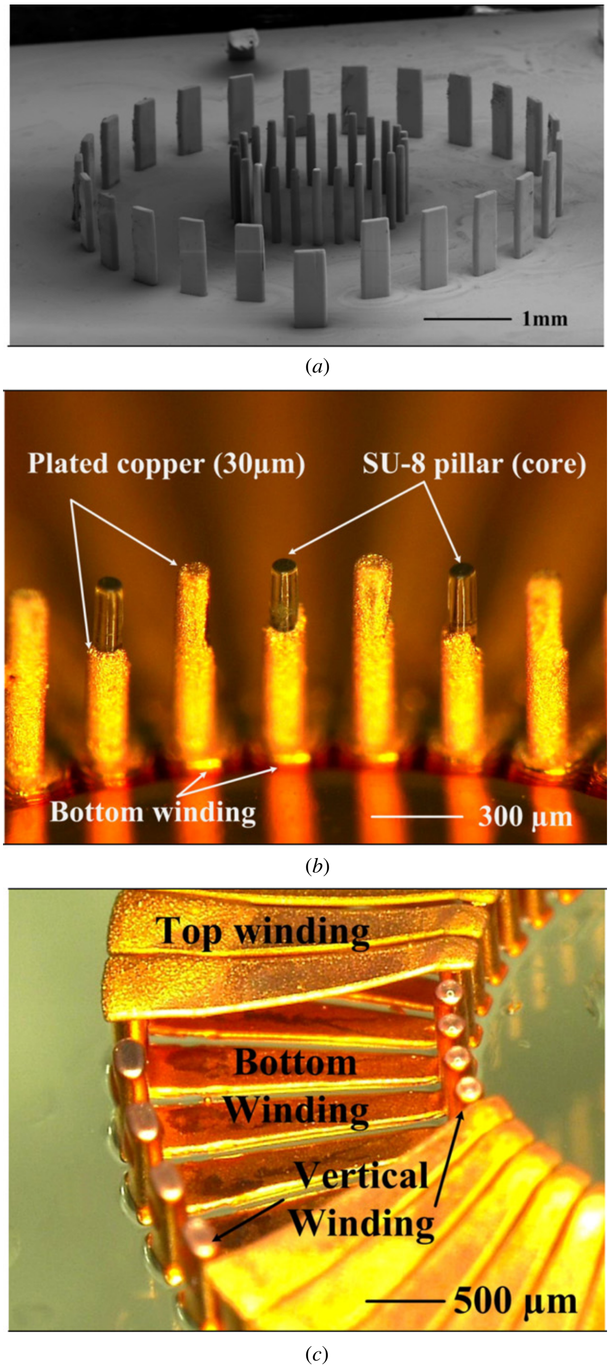

Figure 3. Images of partially completed samples at various fabrication steps (SEM image; Hitachi S-3700N, Optical image; Keyence VHX-600 Digital Microscope): (*a*) SEM image of high aspect ratio micropillar array for vertical winding, (*b*) optical image of SU-8 core and plated copper (partially removed copper at upper portion of pillar), (*c*) optical image of windings (some top windings are intentionally removed).

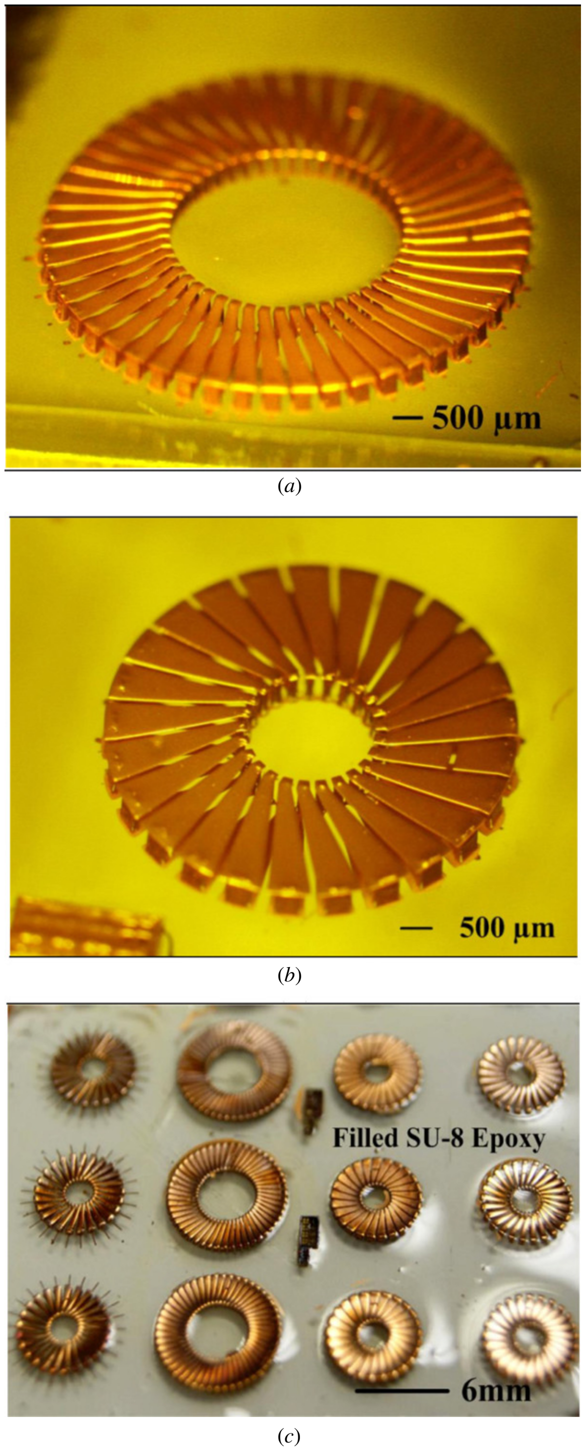

Figure 4. Optical image of a microfabricated toroidal inductor (Keyence VHX-600 Digital Microscope): (*a*) 50-turn toroidal inductor, (*b*) 25-turn toroidal inductor, (*c*) multiple toroidal inductors on a single substrate.

breakdown voltage was investigated by opening the current path between two adjacent windings, thereby allowing a winding-to-winding potential to be applied. Probes were applied to these adjacent windings and a steadily increasing dc voltage was applied until breakdown was observed. Typical breakdown voltages were in excess of 800 V and the failure mechanism was observed to be arcing between conductors in the vicinity of the inner radius. Maximum current capability was investigated by applying current through the windings of the entire inductor by means of probes. An increasing dc current was applied until the windings opened. Typical failure current was approximately 0.5 A without cooling. This current-carrying capability is comparable to other microfabricated inductors previously reported [3, 5].

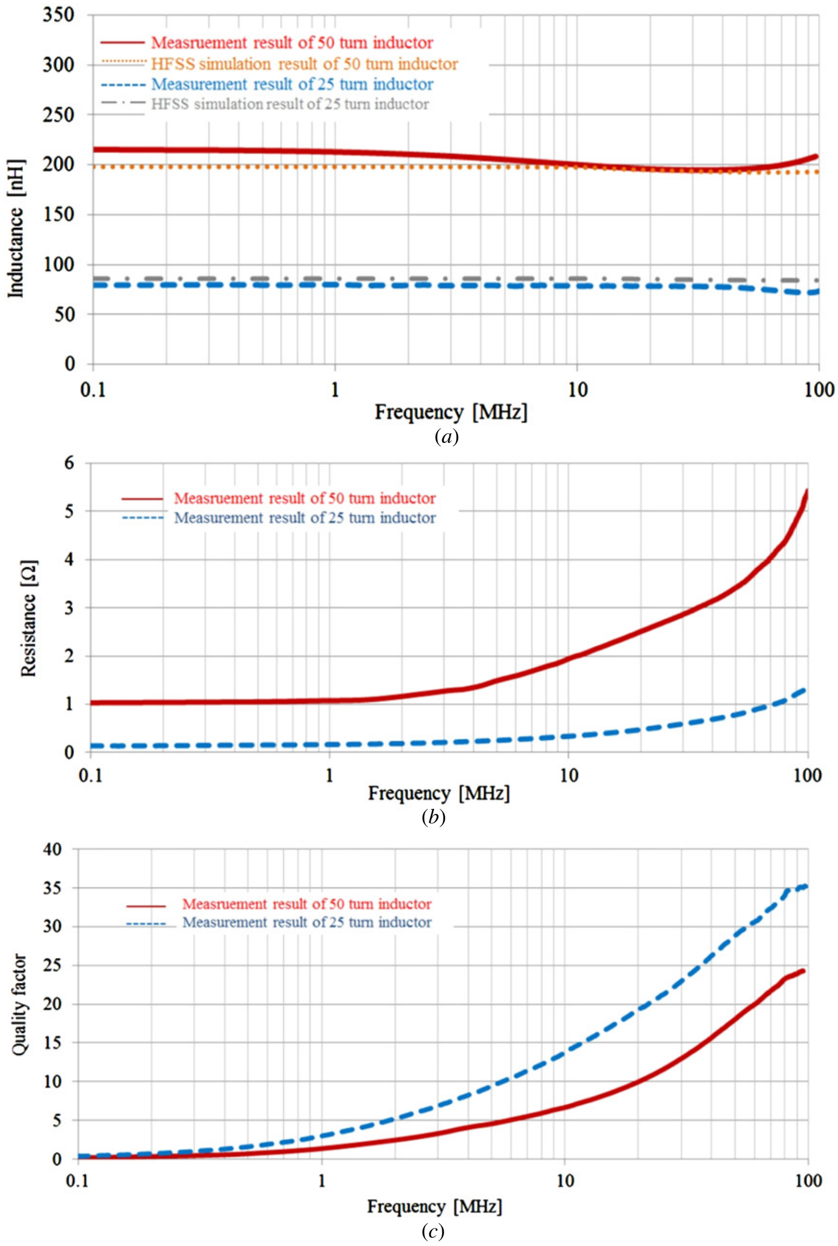

Figure 5. Measurement results of 25- and 50-turn inductors: (*a*) inductance, (*b*) resistance, (*c*) quality factor.

4. Conclusions

A fabrication process for 3-D toroidal inductors with substantial vertical winding extents has been developed. This process has the advantage of being relatively simple with reduced processing time over traditional plate-through-mold approaches. In particular, a dry film process for vertical pillar fabrication and a metal encapsulated polymer core design eliminate 15–20 h softbaking time, and adopting simultaneous metallization on bottom and vertical windings eliminates 8–10 h of bottom-up electroplating. It should be noted that since the metal encapsulation occurs on all sides of the polymer vertical winding, there is no loss of conductor cross-sectional area even though the core of the vertical winding is non-conducting. A solventless, thick sacrificial layer process using non-photopatternable SU-8 pellets has also been introduced as a key enabling step of the fabrication.

The utility of the process has been demonstrated through fabrication of 25- and 50-turn toroidal inductors. These inductors demonstrated inductances of 76 and 200 nH in 0.1–100 MHz, ac resistances of 0.2 and 1 Ω at 0.1 MHz, and quality factors of 35 and 24 at 100 MHz, respectively. HFSS simulation results of inductance for the 25- and 50-turn inductor show good agreement with measured inductance data. We believe these metalized polymer core toroidal inductors could be a candidate for energy storage elements in ultracompact dc–dc converters switching at a high frequency of 30–100 MHz.

Acknowledgments

This work was supported in part by the Advanced Research Projects Agency—Energy (ARPA-E), under contract DE-AR0000123. The authors wish to thank M Araghchini and Professor J H Lang of the Massachusetts Institute of Technology, and D V Harburg and Professor C R Sullivan of Dartmouth College, for valuable technical discussion.

References

[1] Li Q, Lim M, Sun J, Ball A, Ying Y, Lee F and Ngo K 2010 Technology road map for high frequency integrated DC–DC converter *Applied Power Electronics Conf. and Exposition (APEC)* pp 533–9

[2] Lee C, Choi H, Kim Y and Kim N 2011 A low-power CMOS DC–DC buck converter with on-chip stacked spiral inductor *Microelectron. Int.* **28** 38–43

[3] Prabhakaran S, Sun Y, Dhagat P, Li W and Sullivan C 2005 Microfabricated V-groove power inductors for high-current low-voltage fast-transient dc–dc converters *IEEE Power Electronics Specialists Conf.* 1513–9

[4] Sullivan C and Sanders S Design of microfabricated transformers and inductors for high-frequency power conversion *IEEE Trans. Power Electron.* **11** 228–38

[5] O'Donnell T, Wang N, Meere R, Rhen F, Roy S, O'Sullivan D and O'Mathuna C 2008 Microfabricated inductors for 20 MHz dc–dc converters *IEEE Applied Power Electronics Conf. and Exposition* pp 689–93

[6] Meyer C, Bedair S, Morgan B and Arnold D 2010 High-inductance-density, air-core, power inductors, and transformers designed for operation at 100–500 MHz *IEEE Trans. Magn.* **46** 2236–9

[7] Yoon T, Cho W and Kim C 2000 Fabrication of meander and spiral type micro inductors *J. Mater. Sci. Technol.* **16** 236–7

[8] Nakazawa H, Edo M, Katayama Y, Gekinozu M, Sugahara S, Hayashi Z, Kuroki K, Yonezawa E and Matsuzaki K 2000 Micro-DC/DC converter that integrates planar inductor on power IC *IEEE Trans. Magn.* **36** 3518–20

[9] Fukuda Y, Inoue T, Mizoguchi T, Yatabe S and Tachi Y 2003 Planar inductor with ferrite layers for DC-DC converter *IEEE Trans. Magn.* **39** 2057–61

[10] Takeuchi A, Okazaki S, Kobayashi H, Sugawa Y, Takeshima A, Sonehara M, Matsushita N and Sato T 2011 Fabrication of planar power inductor for embedded passives in LSI package for hundreds megaherts switching DC–DC buck converter *IEEE Trans. Magn.* **47** 3204–7

[11] Cheng K and Evans P 1994 Calculation of winding losses in high-frequency toroidal inductors using single strand conductors *IEEE Electr. Power Appl.* **141** 52–62

[12] Orlando B, Royet A and Viala B 2006 Fast analysis of proximity effects in integrated inductors with high permeability magnetic material *IEEE Trans. Magn.* **42** 3371–3

[13] Kuhn W and Ibrahim N 2001 Analysis of current crowding effects in multiturn spiral inductors *IEEE Trans. Microw. Theory Tech.* **49** 31–8

[14] Vandi L, Andreani P, Temporiti E, Sacchi E, Bietti I, Ghezzi C and Castello R 2007 A toroidal inductor integrated in a standard cmos process *Analog Integr. Circuits Signal Process.* **50** 39–46

[15] Orlandi S, Allongue B, Blanchot G, Buso S, Faccio F, Fuentes C, Kayal M, Michelis S and Spiazzi G 2011 Optimization of shielded pcb air-core toroids for high efficiency dc-dc converters *IEEE Trans. Power Electron.* **26** 1837–46

[16] Yu X, Kim M, Herrault F, Ji C, Kim J and Allen M 2012 Silicon-embedded 3D toroidal air-core inductor with through-wafer interconnect for on-chip integration *IEEE Micro Electro Mechanical Systems Conf.* pp 325–8

[17] Orlando B, Hida R, Cuchet R, Audoin M, Viala B, Pellissier-Tanon D, Gagnard X and Ancey P 2006 Low-resistance integrated toroidal inductor for power management *IEEE Trans. Magn.* **42** 3374–6

[18] Sullivan C, Li W, Prabhakaran S and Lu S 2007 Design and fabrication of low-loss toroidal air-core inductors *IEEE Power Electronics Specialists Conf.* pp 1754–9

[19] Lu H, Pillans B, Lee J and Lee J 2005 High aspect ratio air core solenoid inductors using improved UV-LIGA process with contrast enhancement material *Microsyst. Technol.* **13** 237–43

[20] Yoon Y, Park J and Allen M 2005 Polymer-core conductor approaches for RF MEMS *J. Microelectromech. Syst.* **14** 886–94

[21] Johnson D, Vogt A, Ahrens G and Dai W 2010 Thick epoxy resist sheets for MEMS manufacturing and packaging *IEEE MEMS 2010 (Hong Kong)* pp 412–5

[22] Kim J, Allen M and Yoon Y 2011 Computer controlled dynamic mode multidirectional UV lithography for 3-D microfabrication *J. Micromech. Microeng.* **21** 035003

[23] Chung C and Allen M 2005 Uncrosslinked SU-8 as a sacrificial material *J. Micromech. Microeng.* **15** 1–5